A physico-chemical investigation of poly(ethylene oxide)-block-poly(L-lysine) copolymer adsorption onto silica nanoparticles

Stéphanie Louguet, Anitha C. Kumar, Gilles Sigaud, Etienne Duguet, Sébastien Lecommandoux, Christophe Schatz

A physico-chemical investigation of poly(ethylene oxide)-*block*-poly(L-lysine) copolymer adsorption onto silica nanoparticles

Stéphanie Louguet [a,b,c], Anitha C. Kumar [a,e], Gilles Sigaud [d], Etienne Duguet [c], Sébastien Lecommandoux [a,b,*], Christophe Schatz [a,b,*]

[a] *Université de Bordeaux/IPB, ENSCBP, 16 Avenue Pey Berland, 33607 Pessac Cedex, France*
[b] *CNRS, Laboratoire de Chimie des Polymères Organiques (UMR5629), Pessac, France*
[c] *CNRS, Université de Bordeaux, ICMCB, 87 Avenue du Dr Albert Schweitzer, 33608 Pessac, France*
[d] *CNRS, Université de Bordeaux, CRPP, 115 Avenue du Dr Albert Schweitzer, 33600 Pessac, France*
[e] *Acharya Nagarjuna University, Nagarjuna Nagar, Guntur 522 510, Andhra Pradesh, India*

A B S T R A C T

The adsorption behavior of poly(ethylene oxide)-*b*-poly(L-lysine) (PEO_{113}-*b*-PLL_{10}) copolymer onto silica nanoparticles was investigated in phosphate buffer at pH 7.4 by means of dynamic light scattering, zeta potential, adsorption isotherms and microcalorimetry measurements. Both blocks have an affinity for the silica surface through hydrogen bonding (PEO and PLL) or electrostatic interactions (PLL). Competitive adsorption experiments from a mixture of PEO and PLL homopolymers evidenced greater interactions of PLL with silica while displacement experiments even revealed that free PLL chains could desorb PEO chains from the particle surface. This allowed us to better understand the adsorption mechanism of PEO-*b*-PLL copolymer at the silica surface. At low surface coverage, both blocks adsorbed in flat conformation leading to the flocculation of the particles as neither steric nor electrostatic forces could take place at the silica surface. The addition of a large excess of copolymer favoured the dispersion of flocs according to a presumed mechanism where PLL blocks of incoming copolymer chains preferentially adsorbed to the surface by displacing already adsorbed PEO blocks. The gradual addition of silica particles to an excess of PEO-*b*-PLL copolymer solution was the preferred method for particle coating as it favoured equilibrium conditions where the copolymer formed an anchor-buoy (PLL-PEO) structure with stabilizing properties at the silica-water interface.

Keywords:
Silica nanoparticles
Diblock copolymer
Poly(L-lysine)
Poly(ethylene oxide)
Adsorption
ITC

1. Introduction

Poly(ethylene glycol) PEG or poly(ethylene oxide) PEO has become an essential component in the design of various colloidal devices for biomedical applications. PEG prolongs the circulation half-life of therapeutic proteins, liposomes or nanoparticles and reduces their immunogenicity by providing a steric barrier against interactions with plasma proteins, opsonins and cells of the mononuclear phagocyte system [1–3]. Strategies to immobilize PEG on colloid surfaces may be classified into covalent and non-covalent approaches. The covalent coupling of PEG on nanoparticles, which basically involves chemical protocols similar to those of proteins PEGylation has been extensively reviewed [4–7]. It usually requires a multi-step synthesis with extended reaction time and often leads to relatively low grafting densities because of steric repulsions between PEG polymer chains unless specific conditions are used, as for instance the grafting of PEG chains under cloud point conditions [5,8,9]. An alternative and more versatile approach to obtain surfaces with a high-density PEG brush is the physisorption of PEG containing copolymers. Block or grafted copolymers afford the opportunity to create unique adsorbed layers with a good control over the density and the thickness via the selective adsorption of one block [10,11]. In this non-covalent approach, the adsorbing block (anchor block) sticks to the surface, while the other is extended into solution (buoy block) [12–14]. The surface of colloids such as metal oxides or polymer latexes being often negatively charged in neutral aqueous environment, the adsorption of copolymers containing PEG and polycationic segments represents an interesting route for grafting PEG onto solid surfaces to reduce bio-adhesion. For instance, Textor and Spencer have extensively studied the adsorption of poly(L-lysine)-*graft*-poly(ethylene glycol) (PLL-*g*-PEG), a copolymer made of PEG chains grafted onto a polycationic PLL backbone, on various metal oxides and the resistance mechanisms to protein adhesion [15–18]. At neutral pH, the positively charged PLL backbone ($pK_a \sim 10.5$) acts as an anchoring group through electrostatic interactions with the surface while PEG side chains stretch into the solution providing both colloidal

* Corresponding authors. Address: Université de Bordeaux/IPB, ENSCBP, 16 Avenue Pey Berland, 33607 Pessac Cedex, France.
E-mail addresses: lecommandoux@enscbp.fr (S. Lecommandoux), schatz@enscbp.fr (C. Schatz).

stability and protein repellence properties. The density of PEG chains at the particle surface can be controlled by the PEG grafting ratio. High resistance to nonspecific protein adsorption from blood serum and cell adhesion are obtained through a proper choice of this ratio. Additionally, PEG chains can be end-functionalized with various ligands such as peptides or biotin groups affording the possibility to create bioactive surfaces [15,16,19].

Surprisingly, linear block copolymers of PEG and PLL (PEG-*b*-PLL) which share obvious structural similarities with PLL-*g*-PEG have been less described as surface modifiers. Recently, Park et al. have improved the gene transduction efficiency of adenovirus by coating them with PLL-*g*-PEG and PEG-*b*-PLL copolymers [20]. The modification with PEG-*b*-PLL showed superior gene expression over PLL-*g*-PEG, possibly due to the formation of a denser layer of PEG blocks at the virus surface. Actually, most of the research on PEG-*b*-PLL applications is carried out in the field of gene delivery where these block copolymers are used for their ability to form polyion complex micelles (PIC) with nucleic acids such as plasmids DNA [21,22] or more recently short interfering RNA molecules [23].

The present work intends to investigate the adsorption mechanisms of PEO-*b*-PLL copolymers onto silica nanoparticles that are a good example of hydrophilic and negatively charged colloids at neutral pH. An interesting feature of this polymer-colloid system is that both PLL and PEO chains have affinity for silica surface. Indeed, positively charged amine groups of PLL can bind silanolate groups through electrostatic interactions while electron donor groups of PEO segments can interact with silanol groups through hydrogen bonding [24–26]. Regarding the quite large field of copolymers at interfaces this situation is rare and to the best of our knowledge Hoogeven et al. were the first to describe the adsorption of a charged block copolymer with two adsorbing blocks [27]. Authors studied the adsorption of a diblock copolymer consisting of uncharged water-soluble dihydroxypropyl methacrylate (HMA) and positively charged dimethylaminoethyl methacrylate (AMA) onto titania and silica surfaces. One could expect that the higher affinity of the charged block with the surface would favour a typical anchor-buoy conformation of the copolymer chains but authors rather evidenced the formation of a mixed layer of both blocks. In this layer, the charged block sticks to the surface, whereas the conformation of the neutral block depends on the amount of space left. Hence, for low adsorbed amounts of copolymer, the neutral block adopts a flat conformation, whereas it can form loops and tails at high adsorbed amounts.

Here, the whole study is intentionally restricted to a limited number of experimental parameters in order to get the most accurate picture of the adsorption mechanisms of the PEO-*b*-PLL copolymer onto silica nanoparticles. Hence, a model linear block copolymer, namely PEO^{113}-*b*-PLL^{10} with a low polydispersity index ($\overline{M_w}/\overline{M_n}$ = 1.1) will be used for adsorption experiments in 100 mM phosphate buffer at pH 7.4. The adsorption of corresponding homopolymer blocks will be also investigated in similar conditions. Using common physico-chemical techniques including adsorption isotherm measurements, dynamic light scattering, microelectrophoresis and isothermal titration calorimetry (ITC), we attempt to answer both questions: how PEO-*b*-PLL copolymers adsorb onto silica particles and how are the particles stabilized?

2. Materials and methods

2.1. Materials

Tetraethoxysilane (TEOS 99%, Aldrich) and ammonium hydroxide (30% in water, Aldrich) were purchased in their reagent grades and used without further purification. Dimethylformamide (DMF) (Scharlau, 99.9%) was dried over CaH_2 and cryodistilled prior to use. Amino-terminated PEO ($\overline{M_n}$ = 5000 g/mol, $\overline{M_w}/\overline{M_n}$ = 1.02) purchased from Rapp Polymere was dissolved in dioxane and lyophilized to remove water traces. ε-trifluoroacetyl L-lysine *N*-carboxyanhydride (TFA L-Lys NCA) (Isochem, +96%) and 4-(2-hydroxy-1-naphthylazo)benzenesulfonic acid sodium salt also referred as acid orange II or C.I. acid orange 7 (Aldrich) were used as received.

2.2. Synthesis and characterization of silica nanoparticles

The synthesis of spherical and size-monodisperse silica nanoparticles was performed following an existing method described in the literature [28]. Briefly, 250 mL of absolute ethanol and 17.7 mL of ammonium hydroxide were introduced in a round flask of 500 mL under stirring at 300 rpm to get a homogeneous mixture. 20 mL of TEOS were rapidly introduced in the medium and the reaction was carried out during 2 h in a bath sonicator filled with cold water. 150 mL of mQ water was added to the reaction mixture, then ammonium hydroxide and ethanol were evaporated and the medium dialyzed against water. The final concentration in silica was determined by thermogravimetric analysis. The hydrodynamic diameter of silica particles in phosphate buffer (7.4, 100 mM) was 82 nm with a polydispersity index of 0.04 as measured by dynamic light scattering (Malvern Nanosizer). The zeta potential was −41 mV ± 5 mV in the same solvent conditions. A surface charge density of −12.7 C/g silica was determined by potentiometric titration of the silica particles according to the procedure described by Sonnefeld et al. [29]. Because the charge density of silica particles is dependent on the ionic strength of the medium, particles were titrated in 0.255 M NaCl to have the same ionic strength as the 0.1 M PB buffer at pH 7.4 that was used throughout the study (see supporting information).

2.3. Polymer and block copolymer synthesis and characterization

Detailed information about the synthesis of PLL homopolymer and PEO-*b*-PLL copolymer as well as characterization procedures can be found in previous references [30,31]. Briefly, PEO-*b*-PLL copolymer was synthesized by ring-opening polymerization (ROP) of TFA L-Lys NCA initiated by an amino end-functionalized PEO macroinitiator. 1-azido-3-aminopropane compound was synthesized following an already published procedure and used as aminated initiator for the synthesis of poly(TFA L-lysine) homopolymer [32,33]. The degree of polymerization ($\overline{DP}$) of the poly(TFA L-lysine) segment within the block copolymer was determined from the molar ratio of TFA lysine and ethylene oxide units obtained by ^{1}H NMR analysis (Brücker AC 400 spectrometer) in deuterated DMSO. For poly(TFA L-lysine) homopolymer, the determination of $\overline{DP}$ by ^{1}H NMR was only possible after deprotection of the trifluoroacetyl groups since in DMSO the peaks of the initiator were hidden by those of the polymer. Molecular weight distribution and polydispersity index (PDI = M_w/M_n) were determined by size-exclusion chromatography performed in DMF with LiBr (1 g/L) at 60 °C as eluent (0.8 mL/min) using a Waters apparatus (Alliance GPCV2000) equipped with a refractometric detector and two PLgel 5 μm Mixed-C columns calibrated with polystyrene standards. The removal of labile trifluoroacetyl (TFA) protecting groups of L-lysine was achieved by treatment with KOH (1.5 equiv.) in THF at room temperature (RT) during 24 h. Once the reaction completed, THF was removed by rotary evaporation and the product precipitated in cold diethyl ether and finally dried overnight under dynamic vacuum (see supporting information). The final structure and composition of both synthesized compounds are depicted in Fig. 1. We will consider in the following a PEO_{113}-*b*-PLL_{10} (PDI = 1.1) copolymer and a PLL_{22} (PDI = 1.2) homopolymer. It is worth noting that both these compounds could not directly be solubilized in

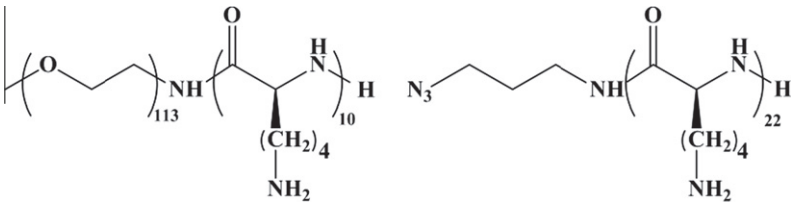

Fig. 1. Structure of synthesized PEO-*b*-PLL copolymer and PLL homopolymer.

100 mM phosphate buffer (PB) at pH 7.4 because of remaining traces of KOH. Therefore, the polymer powder was first dispersed in PB buffer and after overnight stirring the pH was adjusted to 7.4 with a 1 M HCl solution. A potentiometric titration of the copolymer evidenced that the protonation degree of the lysine moieties was close to 100% at pH 7.4. Besides, a $\overline{DP}$ of 9.6 for the lysine block was derived from conductivity measurement, which was in good agreement with NMR analysis (see supporting information).

2.4. Complexation profile of PEO-b-PLL onto silica nanoparticles

Interactions between silica nanoparticles and PEO-*b*-PLL copolymer were monitored by dynamic light scattering (DLS) using an ALV laser goniometer, which consists of a 35 mW HeNe linear polarized laser with a wavelength of 632.8 nm and an ALV-5000/EPP Multiple Tau Digital correlator with 125 ns initial sampling time. Measurements were carried out at a single angle of 90° at 25 °C. 2.5 mL of silica suspension at 21 g/L in 100 mM PB at pH 7.4 were introduced in a 20 mm diameter cylindrical glass cell. Increasing amounts of block copolymer solution in the same buffer were directly added to the silica suspension in the cell. After each addition, the solution was magnetically stirred for 10 min prior to DLS analysis. Data were recorded with the ALV correlator control software, the counting time being set to 60 s for each sample. Mean hydrodynamic diameters were determined using the cumulant analysis method [34]. In the range of polymer/particle ratios that have been investigated, the maximal volume of PEO-*b*-PLL copolymer solution added to silica nanoparticles was 1.25 mL, which corresponded to a final polymer concentration of 5.4 g/L and a dilution factor of 1.5 for the particle suspension.

2.5. Polymer and copolymer adsorption measurements

The adsorption isotherm of PEO-*b*-PLL copolymer on silica nanoparticles (2.8 g/L) was determined in 100 mM PB buffer (pH 7.4). To 700 μL of copolymer in PB varying in concentration, 700 μL of silica suspension at 5.6 g/L were quickly added. After 24 h stirring at RT, nanoparticles were centrifuged (11,092*g*, 30 min, 10 °C) and the supernatant containing free (unadsorbed) copolymer was removed and spectrophotometrically analyzed (see below). Competitive adsorption experiments from PEO/PLL mixtures were performed in the same way. Molar compositions of the mixture were chosen to be the same as for block copolymer adsorption experiments, especially by taking into account that PLL homopolymer is twice larger than PLL block in the copolymer. For the displacement adsorption experiment, silica particles were coated at first by PEO. Two equivalent volumes of PEO solution at 3.55 g/L and silica particles at 8.8 g/L were mixed together to get a final concentration of 0.4 g PEO/g particles, which corresponded to the plateau concentration in the PEO adsorption isotherm on silica particles (see supporting information). After overnight stirring, the excess of PEO was removed by extensive dialysis against 100 mM PB pH 7.4 (5 days, MWCO 50,000 g/mol). The particles were diluted by a factor of 1.6 after dialysis. Also, a residual concentration of 0.6 g/L of PEO was determined and was systematically subtracted to the amount of free PEO determined in the following. Two equivalent volumes of PEO coated silica particles and PLL solution varying in concentration were rapidly mixed together. After 24 h, nanoparticles were centrifuged (11,092*g*, 30 min, 10 °C) and the supernatant was analyzed (see below).

Depending on the type of polymers two different protocols were applied to determine the concentration of free polymer from depleted supernatants. In both competition and displacement studies, size-exclusion chromatography was used to measure the concentration of PEO homopolymer by integrating its eluting peak. The polymer separation was performed on two serially connected Aquagel-OH 30 and 40 columns. The detection was operated by a differential refractometer (Optilab rEX, Wyatt). A degassed 100 mM PB buffer pH 7.4 was used as eluent. The flow rate was maintained at 0.8 mL/min, and the amount of sample injected was 100 μL. A calibration curve was obtained by plotting the area of the PEO eluting peaks *vs.* the concentration of PEO from 0 to 5 g/L (see supporting information). The titration of PLL homopolymer in competition and displacement adsorption studies as well as PEO-*b*-PLL copolymer was carried out spectrophotometrically using an anionic dye, the 4-(4-hydroxy-1-naphthylazo) benzenesulfonic acid (Acid Orange 7) [35,36]. A 10^{-4} M solution of the dye in 1.7×10^{-2} M acetic acid was prepared. A calibration curve was established by mixing 200 μL of polymer solution varying in concentration from 0 to 125 mg/L with 1300 μL of dye solution (see supporting information). After 24 h of stirring, the absorbance of the solution was measured at $\lambda = 485$ nm using a Spectramax M2^e (Molecular Devices) UV–visible spectrophotometer. The concentration of free PLL or PEO-*b*-PLL in supernatants was obtained with the same protocol using the calibration curve. The quite high concentration in acetic acid in the dye solution ensured a full protonation of lysine residues of PLL and PEO-*b*-PLL in supernatants.

2.6. Electrophoretic mobility measurement

The electrophoretic mobility of bare and PEO-*b*-PLL coated silica nanoparticle suspensions ([silica] = 2.8 g/L) was measured as a function of the adsorbed polymer amount using a Malvern ZetaSizer Nano ZS instrument. The electrophoretic mobility (μ) was converted to the zeta potential (ζ) using the Smoluchowski approximation. All the measurements were the average of at least five runs performed at 25 °C.

2.7. TEM and SEM analysis

The surface morphology of bare and hybrid nanoparticles were observed using transmission and scanning electron microscopy (TEM and SEM). TEM images were obtained with a Hitachi H7650 microscope working at 80 kV equipped with a GATAN Orius 10.5 megapixel camera. For the sample preparation, one droplet of the nanoparticle solution ([silica] = 2.8 g/L) was deposited on a copper grid (200 mesh) coated with carbon film. After 1 min, excess liquid was blotted away with a piece of filter paper and grids

were air-dried at room temperature. SEM observations were performed with a JEOL JSM-6700F NT scanning electron microscope operating at 5 kV. 25 μL of particle suspension ([silica] = 0.28 g/L) were deposited on a sample holder, air-dried for 48 h at RT and coated with gold in a cathode evaporator under an argon atmosphere.

2.8. ITC measurements

Microcalorimetric titrations were performed in a NanoITC (TA Instruments). The sample cell (950 μL) was filled with a silica suspension at 4.6 g/L in 100 mM PB buffer at pH 7.4. The syringe was filled with polymer solutions at 1.2 g/L in the same buffer. The first injection was set to a volume of 2 μL followed by 49 injections of 5 μL each at 300-s intervals. The heats of dilution of polymer solutions were determined in blank experiments in which the polymer solutions were injected into the sample cell containing only PB buffer. The dilution heats were then subtracted to obtain the binding heats.

3. Results and discussion

3.1. Adsorption of PEO-b-PLL copolymer onto silica particles

Interactions of PEO-*b*-PLL copolymers with the surface of silica nanoparticles were evaluated by means of dynamic light scattering in 100 mM phosphate buffer (PB) at pH 7.4. At first sight, one could expect that electrostatic interactions between cationic lysine units and anionic silanolate groups might drive their mutual complexation. Therefore, we plotted a complexation profile representing the variation of the normalized hydrodynamic radius (R_H/R_{H0}) where R_{H0} is the radius of the bare particles (R_{H0} = 41 nm) as a function of the molar charge ratio (Z) between cationic and anionic groups (Fig. 2). Potentiometric titration allowed to determine the charge surface of silica particles at pH 7.4 whereas a combination of potentiometry and conductivity measurements were used to correctly evaluate the number of protonated amine groups within the copolymer at pH 7.4 (see supporting information). Importantly, the complexation was performed in a sequential manner, starting from a single suspension of bare silica particles and adding

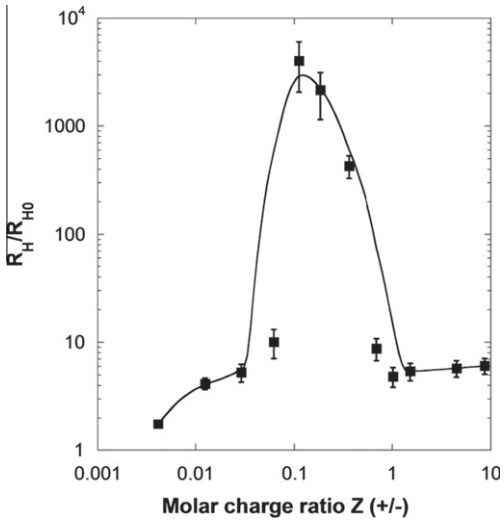

Fig. 2. Variation of the normalized hydrodynamic radius of the silica particles as a function of the amount of added PEO_{113}-*b*-PLL_{10} copolymer expressed in terms of charge ratio between cationic lysine and anionic silanolate groups. Experimental conditions: $[silica]_0$ = 21 g/L, 100 mM phosphate buffer, pH 7.4. The solid line serves to guide the eye only.

increasing amounts of copolymer to reach the next charge ratio. This way of proceeding guarantees the consistency of the R_H/R_{H0} variation, especially when colloidal instabilities leading to particles aggregation occur. The complexation profile evidences that particle sizes are increased even at low charge ratio (Z = 0.01) meaning that a little amount of added block copolymer strongly interacts with the silica surface modifying the particle colloidal state. Fig. 2 also shows a marked particle aggregation starting at low charge ratio (Z = 0.1) followed by a redispersion of the particles from Z = 1. The fact that the system aggregates far below the theoretical isoelectric point (Z = 1) means that non-electrostatic interactions have to be accounted for. Presumably, hydrogen bonding between ether groups of PEO and silanol groups at the silica surface may cause the flocculation at an early stage. The redispersion of particles seems to occur with a remarkable ease from Z = 1 even if they remain aggregated to some extent when an excess of copolymer is added (R_H/R_{H0} = 4.8 at Z = 1). This point is discussed later. TEM and SEM analyses performed on samples at various molar charge ratios confirm the different colloidal states observed by DLS (Figs. 3 and 4).

The profile of complexation clearly evidences two Z-value domains where particles are relatively well stabilized separated from a domain where they flocculate. In order to get a better understanding of copolymer interactions with silica surface, the adsorption isotherm of the copolymer as well as the variation of the potential zeta (ζ) of particles were determined (Fig. 5). The two values of the molar charge ratio, Z = 0.1 and Z = 1, delimiting the flocculation domain are also reported in Fig. 5. The strong decrease of ζ in absolute value at low copolymer concentration originates from ion pairing between SiO^- groups and protonated lysine moieties. However, the adsorption of neutral polymers such as PEO onto charged particles is also known to decrease ζ as the result of an outward displacement of the slipping plane [37]. Thus, the co-adsorption of both blocks most likely explains why particles are almost uncharged at low charge ratios (Z < 1). Interestingly, whereas the variation of ζ flattens out between Z = 0.1 and Z = 1, the plateau onset on the adsorption isotherm is around Z = 1.5, which means that more copolymer is adsorbed without significantly varying the charge surface of silica particles. Indeed, the amount of adsorbed copolymer in the flocculation domain ($0.1 < Z < 1$) is quite high, around 50% of the plateau adsorbed mass. Hence, the formation of large aggregates does not impede further adsorption of copolymer, providing the stirring allows the diffusion of the macromolecules to the particle surface.

From all above experiments, the following mechanism for the adsorption of PEO-*b*-PLL onto silica nanoparticles in phosphate buffer at pH 7.4 may be proposed. At low Z ratios (Z < 0.1), where the block copolymer is in default, both blocks adsorbed onto silica surface, the PLL segment by electrostatic interactions with SiO^- groups and the PEO block through hydrogen bonding with SiOH groups [38]. Copolymer molecules probably have extended, flat conformation due to polymer-substrate interactions as it has been reported for low molecular weight PLL [39] and PEO [40]. The amount of adsorbed copolymer at Z = 0.1 was quite low, about 25% of the plateau concentration in the isotherm, but the zeta potential almost already reached its minimal absolute value. Therefore, this is in agreement with the flat conformation of the adsorbed copolymer molecules as it allows the full coverage of the particle surface with a minimum amount of copolymer. However, this thin layer of copolymer did not prevent the flocculation of particles since neither electrostatic nor steric repulsion forces could stabilize them. As a consequence the system experienced a marked colloidal destabilization with the formation of large particle aggregates (Fig. 3b). When more copolymer was added the flocs start to redisperse, traducing that the conformation of the copolymer at the interface had changed. At this stage where less than 50% of the total mass of copolymer was adsorbed, two possibilities or a

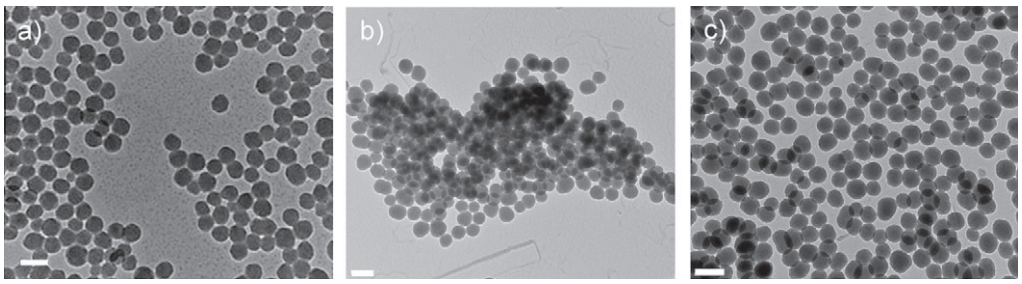

Fig. 3. TEM images of PEO_{113}-*b*-PLL_{10} coated silica particles at different charge ratios: $Z = 0$, bare particles (a), $Z = 0.1$ (b), $Z = 7$ (c) (scale bar: 100 nm).

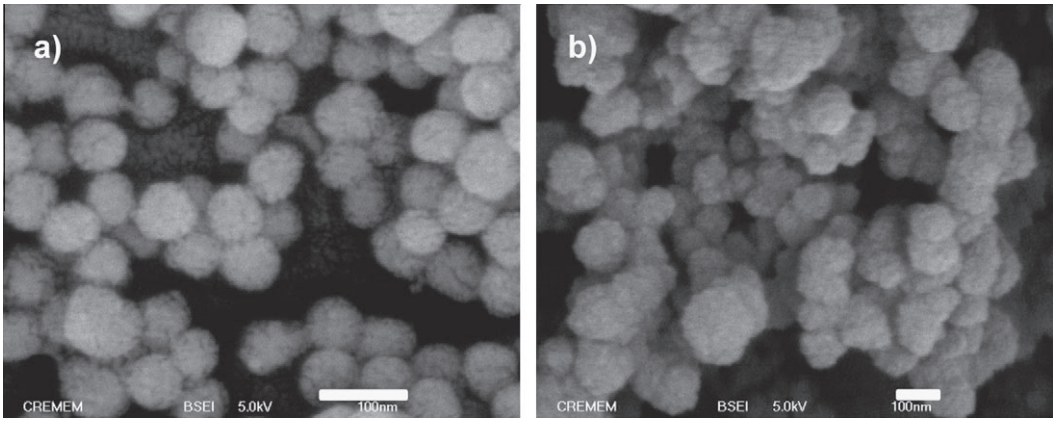

Fig. 4. SEM images of bare silica particles (a) and PEO_{113}-*b*-PLL_{10} coated particles at $Z = 7$ (b) (scale bar: 100 nm).

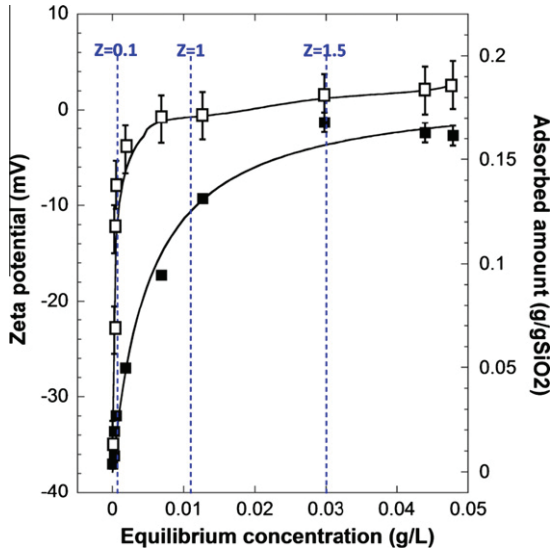

Fig. 5. Adsorption isotherm of PEO_{113}-*b*-PLL_{10} (■) and zeta potential variations of silica nanoparticles (□) as a function of the equilibrium concentration. The onset ($Z = 0.1$) and the end ($Z = 1$) of the flocculation domain are also plotted. Experimental conditions: $[silica]_0 = 2.8$ g/L, 100 mM phosphate buffer, pH 7.4.

combination of them could explain this redispersion. At first, incoming copolymer molecules might adsorb only through their lysine blocks and keep their PEO segments free in solution to provide steric stability. This behavior which assumes a preferential interaction of lysine blocks with silica surface over PEO ones would be also in agreement with the reduced space left at the particle surface. Secondly, new copolymer molecules might also displace already adsorbed PEO segments to some extent. This second hypothesis would suggest that all adsorbed copolymer molecules adopt an anchor-buoy conformation with PLL blocks sticking to the surface and free PEO chains protruding into bulk solution. These two possibilities were independently studied through competitive and displacement adsorption experiments with homopolymers. (see next section).

Despite the strong disaggregation occurring between $Z = 0.1$ and $Z = 1$, the final colloidal state deduced from the profile of complexation remains slightly aggregated ($R_H/R_{H0} = 6$ at $Z = 10$). The main reason of this remanent aggregation has to be correlated to the protocol of particle coating. Actually, the slow and sequential addition of copolymer onto particles forces the system to pass through the isoelectric point (IEP) associated with the flocculation of the particles. Therefore and probably for kinetic reasons, this aggregation state is not fully reversible in a reasonable time even in the presence of an excess of copolymer. This hypothesis was verified by comparing the two possible orders of addition of components. Hydrodynamic sizes and polydispersity indexes of copolymer coated particles were determined for various Z ratios ($Z > 1$) either by slowly adding the copolymer to the particles (addition order 1, as for the profile of complexation) or the opposite (addition order 2) (Table 1). The particles were stable whatever the order of addition but a significant difference in the degree of aggregation was observed. The addition of copolymer to particles systematically led to higher sizes and polydispersity indexes since the system experienced a flocculation state before its redispersion. Conversely, when particles were added to an excess of copolymer the IEP was quickly bypassed and the particles were almost not aggregated. It is also believed that this order of addition should allow the preferential adsorption of PLL blocks over PEO blocks, hence favoring the anchor-buoy copolymer conformation at the particle surface.

Table 1
Hydrodynamic diameters and polydispersity indexes (PDI) of silica particles coated with PEO_{113}-*b*-PLL_{10} at different molar charge ratios ($Z = \pm$). The copolymer was added to the particle solution (addition order 1) or the particles were added to the copolymer in excess (addition order 2). Experimental conditions: $[silica]_0 = 2.8$ g/L, 100 mM phosphate buffer, pH 7.4.

		D_H (nm)	PDI
Bare silica particles		82	0.04
PEO-b-PLL coated silica particles			
$Z \approx 4$	Addition order 1	179	0.19
	Addition order 2	130	0.13
$Z \approx 6$	Addition order 1	158	0.18
	Addition order 2	122	0.12
$Z \approx 10$	Addition order 1	148	0.17
	Addition order 2	120	0.13

3.2. Adsorption of homo-PEO and homo-PLL onto silica particles: competitive and displacement experiments

Competitive and displacement adsorption experiments performed with PEO_{113} and PLL_{22} homopolymers may provide additional information on the copolymer adsorption mechanism, especially in the flocculation domain where the conformation of adsorbed copolymer is supposed to evolve. Such experiments are well documented in the literature, but mostly deal with the adsorption of different molecular weight fractions of a same polymer. It was established that high molecular weight polymers adsorb preferentially and can displace lower ones initially adsorbed [41–44]. For polyelectrolytes, a high ionic strength is required to promote the exchange of small molecules by larger ones while at low ionic strength the exchange rate is low and the adsorbed layer is mostly composed of small molecules [45–49]. Only a few studies deal with competitive and/or displacement experiments with chemically different polymers such as two neutral homopolymers [40,50], two polyelectrolytes [49] or a neutral polymer and a polyelectrolyte [51–53]. The number and strength of segment-surface contacts per chains as well as the charge density and the ionic strength in case of polyelectrolytes are the main parameters determining the exchangeability in the adsorption layer [53].

Competitive adsorption experiments were carried out by adsorbing increasing concentrations of a mixture of PEO and PLL homopolymers in the same molar ratio as in the copolymer, namely a 1:1 M composition (Fig. 6a). We assume that the small difference in PLL block length in the homopolymer (PLL_{22}) and the copolymer (PEO_{113}-*b*-PLL_{10}) is negligible considering the quite high DP of the PEO block. Especially, one may expect that both PLL_{10} and PLL_{22} block adsorb in flat conformation at silica surface [39]. Each point in Fig. 6a corresponds to an independent experiment performed in same conditions as for the adsorption isotherm of the copolymer. This allows us to mimic to some extent the copolymer adsorption from the behavior of a homopolymer mixture. Fig. 6a shows that both PEO and PLL chains adsorbed with a high affinity at low concentrations of the mixture ($C_{mix,eq} < 0.005$ g/L), the higher amount of adsorbed PEO being simply related to the initial composition of the homopolymer mixture. In this range of concentrations, particles already flocculated (results not shown), which indicates that both polymers probably adsorbed in a flat conformation without any capacity of colloidal stabilization through overcharging or steric effects as mentioned before [54]. At higher concentrations ($C_{mix,eq} > 0.02$ g/L), PLL was preferentially adsorbed and almost no adsorption of PEO occurred at $C_{mix,eq} = 0.22$ g/L, which denotes a higher affinity of PLL blocks for the silica surface. Interestingly, the amount of adsorbed PEO steadily decreased while the amount of adsorbed PLL increased. Therefore, in addition to SiO^- groups, PLL can bind to the same adsorbing sites of PEO (silanol groups) with a higher interaction strength. Hydrogen bonding between carbonyl functions located on the polypeptide backbone and silanols is most likely at the origin of this strong binding. For instance, it has been reported that PLL adsorbs on silica at pH 4 where the dissociation of the silanol groups is negligible, provided the ionic strength of the medium is not too low (>10 mM) [55,56].

Extrapolating the above results to the copolymer adsorption, this competitive experiment confirms that both blocks stick to the surface at low copolymer concentration ($C_{copo,eq} < 0.005$ g/L) leading to the flocculation of particles (Figs. 2 and 6). At higher concentrations the preferential adsorption of PLL over PEO indicates that the block copolymer must progressively adsorb trough its lysine block, which is in line with the first hypothesis previously stated. This also demonstrates that the copolymer must adopt an anchor-buoy conformation when particles are added to an excess of copolymer solution (Table 1, addition order 2). A quite high concentration of copolymer should be required ($C_{copo,eq} = 0.22$ g/L which is equivalent to $Z = 2.9$) to fully cover the particles solely

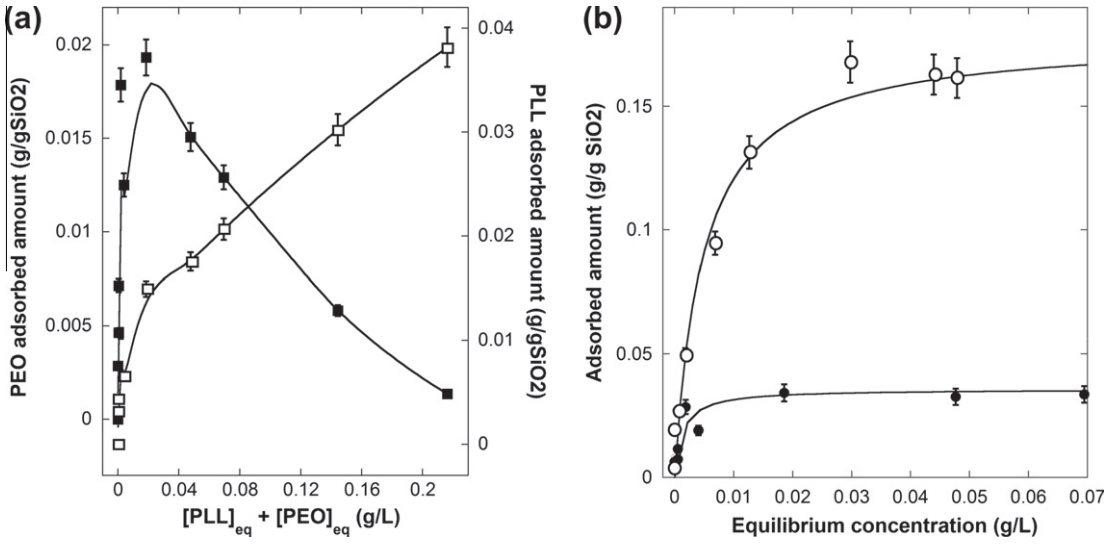

Fig. 6. (a) Competitive adsorption of PEO_{113} (■) and PLL_{22} (□) homopolymers from a PEO_{113}:PLL_{22} mixture (1:1 M ratio). (b) Adsorption isotherms of PEO_{113}-*b*-PLL_{10} copolymer (○) and an equimolar mixture of homopolymers (●). Experimental conditions: $[silica]_0 = 2.8$ g/L, 100 mM phosphate buffer, pH 7.4. The solid lines serve to guide the eye only.

with PLL blocks. Another way to analyze the results from the competitive experiment is to compare adsorption isotherms of block copolymer and mixture of homopolymers (Fig. 6b). At low concentrations, both isotherms overlap confirming that both blocks of the copolymer are adsorbed in a flat conformation like homopolymers. By increasing the surface coverage, the amount of adsorbed copolymer gets higher than this of the homopolymer, which demonstrates that the copolymer chains become adsorbed through their lysine blocks, PEO blocks being less and less adsorbed. Considering that PLL blocks are completely stuck to the silica surface at the isotherm plateau, one calculates that 3.0×10^{-4} and 2.6×10^{-4} mole of lysine residues (M = 128 g/mol) is adsorbed per gram of particles for PLL and block copolymer, respectively. This is a strong indication that both lysine blocks indeed adopt a similar flat conformation. The slight difference might be due to the steric hindrance caused by non-adsorbing PEO blocks of the copolymer that limit the accessibility of incoming lysine blocks to the surface.

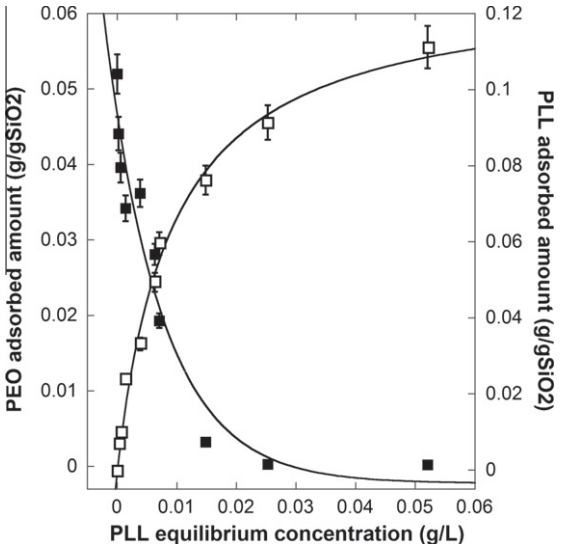

Fig. 7. Displacement adsorption behavior of PEO_{113} by addition of PLL_{22} on PEO_{113} precoated silica particles. Residual concentrations of PEO at silica surface (■) and adsorbed concentrations of PLL (□) are determined at different concentrations of PLL. Experimental conditions: $[silica]_0$ = 1.73 g/L, 100 mM phosphate buffer, pH 7.4. The solid lines serve to guide the eye only.

The competitive experiment evidenced the preferential adsorption of PLL blocks over PEO ones, but did not demonstrate the occurrence of PEO desorption (hypothesis 2). In order to test this hypothesis, increasing concentrations of PLL were added on silica particles precoated with PEO. The amounts of adsorbed PLL and desorbed PEO were independently determined (see Section 2). Fig. 7 unambiguously shows the exchangeability between adsorbed PEO chains and added PLL molecules. All PEO chains are desorbed from the surface at $C_{PLL,eq}$ = 0.055 g/L. This confirms the much higher interaction strength of PLL over PEO and also suggests that a similar behavior should occur with the block copolymer. For the overall displacement adsorption, one calculates that ~ 4 PLL chains adsorb for one PEO chain that desorbs. This supports the hypothesis that PLL chains not only adsorb through electrostatic interactions with SiO^- groups but also by hydrogen bonds with silanol groups initially bound to PEO residues.

3.3. Microcalorimetry study

Isothermal titration calorimetry (ITC) was used to quantify adsorption energies of PEO, PLL and PEO-*b*-PLL with silica particles (Fig. 8). All experiments were performed by slowly adding polymer solutions to the silica suspension in the sample cell. Therefore, this reproduced the conditions previously used for the complexation profile (Fig. 2). ITC is an effective technique to determine relevant thermodynamic parameters (ΔH, ΔS, ΔG, K_B) from the adsorbed or released heat due to interactions between components. The determination of the thermodynamic parameters by a fitting procedure requires to know the number of binding sites on both the polymer and at the particle surface. As multiple interactions may occur between polymer chains and colloid surface, this number is not easy to evaluate. The situation is even complicated by charge regulation effects causing a modification of the surface charge upon adsorption of polyelectrolytes [57]. In a recent work on polymer adsorption onto silica particles, Chiad et al. simply considered the molar ratio between polymer and SiO_2 [58]. Beyond the difficulty to correctly evaluate the number of active sites, the flocculation of the particles when the polymer or block copolymer was slowly added to the particle suspension was a major concern. For all previous experiments the stirring speed was fast enough to maintain the flocs in a dispersed state and therefore the accessibility of the polymer chains to the surface was not really affected. The situation is rather different in the ITC instrument since the stirring speed was low and the size of the stirrer quite small. We simulated the PEO adsorption onto silica particles in a transparent 2 mL

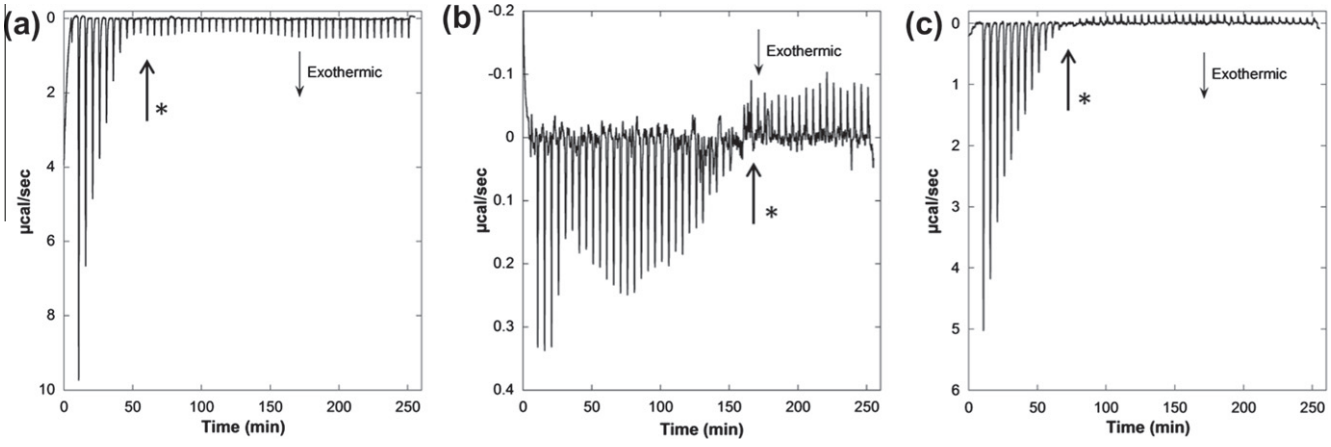

Fig. 8. ITC thermograms of polymer adsorption on silica nanoparticles: PEO_{113} (a), PLL_{22} (b), PEO_{113}-*b*-PLL_{10} (c). Experimental conditions: $[silica]_{cell}$ = 4.6 g/L, $[polymer]_{syringe}$ = 1.2 g/L, 100 mM phosphate buffer, pH 7.4. The arrows with an asterix (∗) show the onset of the plateau used to derive the polymer concentrations in Table 2.

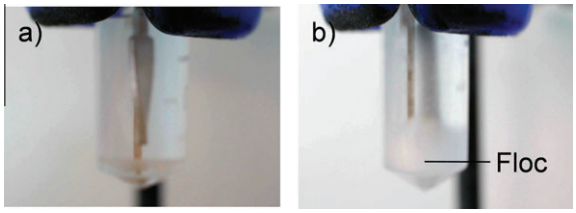

Fig. 9. PEO adsorption onto silica particles using same sample volume and stirring conditions as in the ITC instrument. Snapshots were taken before (a) and immediately after (b) addition of 100 µL of 1.2 g/L PEO solution onto silica suspension (4.6 g/L).

microtube using the same tiny paddle stirrer and stirring speed as in the ITC instrument (Fig. 9). We clearly noticed that particles quickly flocculated upon addition of PEO evidencing that stirring conditions were not strong enough to maintain the flocs in suspension and to allow the diffusion of polymer chains to the interface. As a consequence ITC thermograms reached a plateau for PEO, PLL and PEO-*b*-PLL concentrations far below to those found at the plateau on adsorption isotherms (Table 2).

In these conditions, ITC measurements were exploited by considering the heat released at the early stage of the adsorption process when it may be assumed that all polymer or copolymer chains were adsorbed at silica surface as indicated by the high affinity adsorption isotherms found for PEO, PLL and PEO-*b*-PLL (Figs. 5 and 6a). Therefore, the change in enthalpy upon adsorption of polymers onto silica surface was derived from the integration of the second peak on thermograms (Figs. 8), the intensity of the first peak being insignificant due to the long delay prior to equilibration and the ensuing diffusion from the top of the syringe to the cell. For PEO_{113} the enthalpy of adsorption per residue is negative as expected for a mechanism driven by hydrogen bonding (Table 3). However, the enthalpy, in absolute value, is rather low compared to the typical energy of a hydrogen bond (10–50 kJ/mol) indicating that only a fraction of ethylene oxide residues (5–25%) bind to silanol groups. This result can be explained by considering that the full adsorption of PEO chains would considerably reduced their configurational (translational) entropy. Hence, even lower adsorption enthalpies should be measured with PEO of lower molecular weights as the loss in configurational entropy is supposed to increase when polymer chains get shorter [59]. As a matter of fact adsorption enthalpies of 1.8 and 0.1 kJ/mol per ethylene oxide residues were determined in similar conditions with PEO of 2000 and 300 g/mol, respectively (data not shown). For PLL_{22}, the very low enthalpy of adsorption per lysine residues was unexpected with regard to displacement and competitive adsorption experiments that have shown the preferential adsorption of PLL over PEO. Therefore, this supports the occurrence of substantial entropic effects related to the release of counterions or water molecules upon interaction of PLL chains with silica surface. In terms of electrostatic interactions the adsorption of polyelectrolyte chains onto oppositely charged surface is similar to the complexation of oppositely charged polyelectrolytes. In the latter case, it is known that the increase in entropy largely drives the complexation for highly charged polyelectrolytes [60]. Recently, in a study on the thermodynamics of plasmid DNA condensation by PEO-*b*-PLL copolymers,

Table 2
Polymer concentrations at the plateau onset in ITC and adsorption isotherm experiments.

	Polymer concentrations[a] (g polymer/g particles)	
	ITC[b]	Adsorption isotherms
PEO_{113}	0.016	0.96[c]
PLL_{22}	0.042	0.37[c]
PEO_{113}-*b*-PLL_{10}	0.018	0.18[d]

[a] The values refer to initial (added) polymer concentrations and not to equilibrium concentrations.
[b] See arrows in Fig. 8.
[c] See Supporting Information.
[d] See Fig. 5.

Table 3
Enthalpy of polymer adsorption derived from the heat released at the second injection in ITC measurements (Values derived from literature are mentioned in brackets).

Polymer	$\Delta H_{adsorption}$ (kJ/mol monomer)
PEO_{113}	−2.5 (−3 [62] and −2.5 [63])
PLL_{22}	−0.2 (−1 [64])
PEO_{113}-*b*-PLL_{10}	−1.5

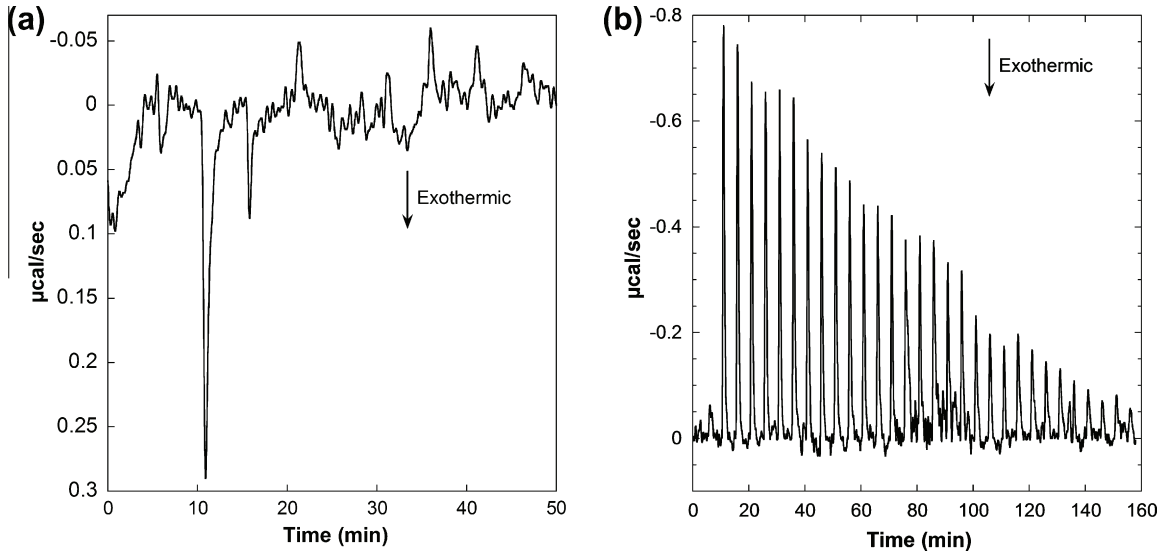

Fig. 10. Displacement adsorption experiments followed by ITC. Titration of PLL coated silica particles by PEO (a). Titration of PEO coated particles by PLL (b). Experimental conditions: $[silica]_{cell}$ = 4.6 g/L, $[polymer]_{syringe}$ = 1.2 g/L, 100 mM phosphate buffer, pH 7.4.

Kim et al. reported positive enthalpies of complexation (+0.08 kJ/mol lysine for PEO_{273}-*b*-PLL_{20} in 100 mM NaCl), the condensation being driven by large negative values of $T\Delta S$ [22]. Here, the slight exothermicity measured upon PLL adsorption on silica particles may reflect the contribution of hydrogen bonds in addition to electrostatic interactions. Fig. 8 also shows two distinct regimes of PLL adsorption which may correspond to two different polymer layers: a first one where PLL chains are tightly bound to the surface through ions pairing and a second one where PLL has the possibility to form some loops and tails [61]. Considering that block copolymers adsorb in a similar fashion as homopolymers, which is expected at the very beginning of the particle titration, the theoretical value of the adsorption should be −2.3 kJ/mol. The lower actual value (−1.5 kJ/mol) suggests that lysine blocks hinder the full adsorption of PEO blocks to some extent (Table 3).

Displacement adsorption experiments with PEO and PLL homopolymers were also conducted on ITC in a similar manner as described previously (Fig. 10). In a first step, silica particles were coated by PLL or PEO by adding the right amount of homopolymer to get the plateau concentration on adsorption isotherms. In a second step, PEO or PLL polymer, respectively, was slowly added to the particle suspension. Interactions of PEO with PLL coated particles were almost negligible since only a single peak of low intensity was detected at the first injection (Fig. 10a). Conversely, Fig. 10b shows that interactions of PLL chains with PEO coated particles were endothermic (ΔH = +0.7 kJ/mol of PLL residues), which is in line with an entropy driven desorption of PEO chains. This indicates that added PLL could indeed displace adsorbed PEO chains despite the initial aggregated state of the particles, hence confirming the high affinity of PLL with silica surface.

4. Conclusion

The adsorption behavior of PEO_{113}-*b*-PLL_{10} copolymer at the surface of silica nanoparticles has been investigated from the adsorption behavior of PEO_{113} and PLL_{22}. Both homopolymers easily adsorb onto silica, PEO through hydrogen bonding with silanol groups and PLL through a combination of electrostatic interactions as well as hydrogen bonds involving carbonyl groups in the polypeptide backbone. However, competitive and displacement adsorption experiments clearly support the preferential adsorption of PLL despite its much lower degree of polymerization compared to PEO. It is proposed that entropic effects related to the release of counterions upon complexation of PLL with SiO^- groups favour its adsorption. PEO and PLL probably adsorb in a relatively flat conformation owing to their relatively low molecular weight and strong interactions with silica. As a consequence, PLL and PEO coated particles are unstable from a colloidal viewpoint and a marked flocculation was noticed in each case. Thanks to these data, the behavior of PEO_{113}-*b*-PLL_{10} coated particles may be better understood. The striking point is the order of addition of the components. When particles are added in an excess of copolymer, a rapid saturation of the surface by PLL blocks may favour a typical anchor-buoy (PLL-PEO) conformation of the copolymer at the interface and therefore an improved colloidal stability through steric forces. When the block copolymer solution is gradually added to the particle suspension, both blocks have the possibility to adsorb in flat conformation in a similar fashion to homopolymers. As the formation of a thin layer of copolymer at the particle surface does not prevent the flocculation, the particles are rapidly destabilized. The return to a colloidal state can be achieved by adding an excess of copolymer since lysine blocks progressively desorb PEO blocks. However, the system remains aggregated to some extent, which evidences that the flocculation is not completely reversible in these conditions. True equilibrium conformations as those probably obtained by adding the particles to the copolymer might only be achieved in presence of a very large excess of copolymer [63]. Hence, the first way to proceed is definitively the best one with regard to the colloidal behavior of the copolymer coated particles and their use for various applications.

Acknowledgments

This work has been supported by French Research National Agency (ANR) through TecSan 2006 (Nano-Bio Imaging, ANR-06-TecSan-015-03) and Blanc 2007 (ITC-NanoProbe, ANR-07-BLAN-0290-01) programs. We thank Stephane Mornet for helpful discussions and technical assistance.

Appendix A. Supplementary material

Supplementary data associated with this article can be found, in the online version, at doi:10.1016/j.jcis.2011.03.093.

References

[1] G. Storm, S.O. Belliot, T. Daemen, D.D. Lasic, Adv. Drug Deliv. Rev. 17 (1995) 31.
[2] U. Wattendorf, H.P. Merkle, J. Pharm. Sci. 97 (2008) 4655.
[3] K. Knop, R. Hoogenboom, D. Fischer, U. Schubert, Angew. Chem., Int. Ed. 49 (2010) 6288.
[4] D. Bhadra, S. Bhadra, P. Jain, N.K. Jain, Pharmazie 57 (2002) 5.
[5] C. Delgado, G.E. Francis, D. Fisher, Crit. Rev. Ther. Drug Carr. Syst. 9 (1992) 249.
[6] M. Hamidi, A. Azadi, P. Rafiei, Drug Delivery 13 (2006) 399.
[7] J.M. Harris, R.B. Chess, Nat. Rev. Drug Discovery 2 (2003) 214.
[8] P. Kingshott, H. Thissen, H.J. Griesser, Biomaterials 23 (2002) 2043.
[9] J.L. Dalsin, L. Lin, S. Tosatti, J. Vörös, M. Textor, P.B. Messersmith, Langmuir 21 (2004) 640.
[10] L. Qi, J.-P. Chapel, J.-C. Castaing, J. Fresnais, J.-F. Berret, Soft Matter 4 (2008) 577.
[11] J.-F.o. Berret, K. Yokota, M. Morvan, R. Schweins, J. Phys. Chem. B 110 (2006) 19140.
[12] G. Hadziioannou, S. Patel, S. Granick, M. Tirrell, J. Am. Chem. Soc. 108 (1986) 2869.
[13] H.J. Taunton, C. Toprakcioglu, J. Klein, Macromolecules 21 (1988) 3333.
[14] M. Tirrell, S. Patel, G. Hadziioannou, Natl. Acad. Sci. USA 84 (1987) 4725.
[15] N.-P. Huang, J. Vörös, S.M. De Paul, M. Textor, N.D. Spencer, Langmuir 18 (2001) 220.
[16] S. Tosatti, S.M.D. Paul, A. Askendal, S. VandeVondele, J.A. Hubbell, P. Tengvall, M. Textor, Biomaterials 24 (2003) 4949.
[17] S. Pasche, J. Vörös, H.J. Griesser, N.D. Spencer, M. Textor, J. Phys. Chem. B 109 (2005) 17545.
[18] G.L. Kenausis, J. Voros, D.L. Elbert, N. Huang, R. Hofer, L. Ruiz-Taylor, M. Textor, J.A. Hubbell, N.D. Spencer, J. Phys. Chem. B 104 (2000) 3298.
[19] S. VandeVondele, J. Vörös, J.A. Hubbell, Biotechnol. Bioeng. 82 (2003) 784.
[20] J.W. Park, H. Mok, T.G. Park, J. Controlled Release 142 (2010) 238.
[21] K. Itaka, K. Yamauchi, A. Harada, K. Nakamura, H. Kawaguchi, K. Kataoka, Biomaterials 24 (2003) 4495.
[22] W. Kim, Y. Yamasaki, W.-D. Jang, K. Kataoka, Biomacromolecules 11 (2010) 1180.
[23] J. DeRouchey, C. Schmidt, G.F. Walker, C. Koch, C. Plank, E. Wagner, J.O. Rädler, Biomacromolecules 9 (2008) 724.
[24] B. Wind, E. Killmann, Colloid Polym. Sci. 276 (1998) 903.
[25] Z. Fu, M.M. Santore, Langmuir 13 (1997) 5779.
[26] Z. Fu, M.M. Santore, Colloids Surf., A 135 (1998) 63.
[27] N.G. Hoogeveen, M.A.C. Stuart, G.J. Fleer, Faraday Discuss 98 (1994) 161.
[28] C.A.R. Costa, C.A.P. Leite, F. Galembeck, J. Phys. Chem. B 107 (2003) 4747.
[29] J. Sonnefeld, A. Göbel, W. Vogelsberger, Colloid Polym. Sci. 273 (1995) 926.
[30] W. Agut, A. Brulet, D. Taton, S. Lecommandoux, Langmuir 23 (2007) 11526.
[31] J. Rodriguez-Hernandez, M. Gatti, H.-A. Klok, Biomacromolecules 4 (2003) 249.
[32] B. Carboni, A. Benalil, M. Vaultier, J. Org. Chem. 58 (1993) 3736.
[33] W. Agut, R. Agnaou, S. Lecommandoux, D. Taton, Macromol. Rapid Commun. 29 (2008) 1147.
[34] D.E. Koppel, J. Chem. Phys. 57 (1972) 4814.
[35] B.D. Gummow, G.A.F. Roberts, Makromol. Chem. 186 (1985) 1239.
[36] G.G. Maghami, G.A.F. Roberts, Makromol. Chem. 189 (1988) 2239.
[37] L.K. Koopal, V. Hlady, J. Lyklema, J. Colloid Interface Sci. 121 (1988) 49.
[38] S. Mathur, B.M. Moudgil, J. Colloid Interface Sci. 196 (1997) 92.
[39] H.M. Eckenrode, H.L. Dai, Langmuir 20 (2004) 9202.
[40] M. Kawaguchi, A. Sakai, A. Takahashi, Macromolecules 19 (1986) 2952.
[41] G.J. Howard, S.J. Woods, Polym. Sci., Part B: Polym. Phys. 10 (1972) 1023.
[42] C.V. Linden, R.V. Leemput, J. Colloid Interface Sci. 67 (1978) 63.
[43] K. Furusawa, K. Yamashita, K. Konno, J. Colloid Interface Sci. 86 (1982) 35.
[44] M.A. Cohen Stuart, G.J. Fleer, B.H. Bijsterbosch, J. Colloid Interface Sci 90 (1982) 310.
[45] A.W.M. de Laat, G.L.T. van den Heuvel, Colloids Surf., A. 98 (1995) 53.

[46] A.W.M. de Laat, G.L.T. van den Heuvel, M.R. Böhmer, Colloids Surf. A. 98 (1995) 61.
[47] D.R. Bain, M.C. Cafe, I.D. Robb, P.A. Williams, J. Colloid Interface Sci. 88 (1982) 467.
[48] R. Ramachandran, P. Somasundaran, J. Colloid Interface Sci. 120 (1987) 184.
[49] U.S. Adam, I.D. Robb, J. Chem. Soc. Faraday Trans. 1 79 (1983) 2745.
[50] G.P. Van der Beek, M.A.C. Stuart, T. Cosgrove, Langmuir 7 (1991) 327.
[51] A.W.M. de Laat, G.L.T. van den Heuvel, Colloids Surf. A. 70 (1993) 179.
[52] M. Kawaguchi, H. Kawaguchi, A. Takahashi, J. Colloid Interface Sci. 124 (1988) 57.
[53] N.G. Hoogeveen, M.A.C. Stuart, G.J. Fleer, J. Colloid Interface Sci. 182 (1996) 146.
[54] M.A. Cohen Stuart, T. Cosgrove, B. Vincent, Adv. Colloid Interface Sci. 24 (1985) 143.
[55] B.C. Bonekamp, J. Lyklema, J. Colloid Interface Sci. 113 (1986) 67.
[56] M. Jiang, I. Popa, P. Maroni, M. Borkovec, Colloids Surf., A 360 (2010) 20.
[57] J.K. Wolterink, L.K. Koopal, M.A.C. Stuart, W.H. Van Riemsdijk, Colloids Surf., A 291 (2006) 13.
[58] K. Chiad, S.H. Stelzig, R. Gropeanu, T. Weil, M. Klapper, K. Müllen, Macromolecules 42 (2009) 7545.
[59] Z. Fu, M.M. Santore, Langmuir 14 (1998) 4300.
[60] Z. Ou, M. Muthukumar, J. Chem. Phys. 124 (2006) 154902.
[61] B.C. Bonekamp, Colloids Surf 41 (1989) 267.
[62] P. Trens, R. Denoyel, Langmuir 9 (1993) 519.
[63] F. Lafuma, K. Wong, B. Cabane, J. Colloid Interface Sci. 143 (1991) 9.
[64] J.K. West, R. Latour, L.L. Hench, J. Biomed. Mater. Res., Part A 37 (1997) 585.